MOL #62356

Human Carboxylesterase 1 Stereoselectively Binds the Nerve Agent Cyclosarin and Spontaneously Hydrolyzes the Nerve Agent Sarin

Andrew C. Hemmert, Tamara C. Otto, Monika Wierdl, Carol C. Edwards, Christopher D. Fleming, Mary MacDonald, John R. Cashman, Philip M. Potter, Douglas M. Cerasoli, and Matthew R. Redinbo

Departments of Chemistry (M.R.R.) and Biochemistry and Biophysics (A.C.H., C.D.F., M.R.R), University of North Carolina at Chapel Hill, Chapel Hill, North Carolina; U.S. Army Medical Research Institute of Chemical Defense (T.C.O., D.M.C.), Aberdeen Proving Ground, Maryland; Human BioMolecular Research Institute (M.M., J.R.C.), San Diego, California; Department of Molecular Pharmacology (M.W., C.C.E., P.M.P.), St. Jude Children's Research Hospital, Memphis, Tennessee

Molecular Pharmacology Fast Forward. Published on January 5, 2010 as DOI: 10.1124/mol.109.062356
This article has not been copyedited and formatted. The final version may differ from this version.

MOL #62356

Running Title: **hCE1 Stereoselectivity for Nerve Agents**

* Corresponding author: Department of Chemistry, CB #3290, University of North Carolina at Chapel Hill, Chapel Hill, NC 27599-3290. Tel: (919) 843-8910. Fax (919) 962-2388. E-mail: redinbo@unc.edu

Number of text pages: 38

Number of tables: 1

Number of figures: 7

Number of references: 40

Number of words in *Abstract*: 250

Number of words in *Introduction*: 743

Number of words in *Discussion*: 1320

Abbreviations: OP, organophosphorus; sarin, *O*-isopropyl methylphosphonofluoridate; tabun, ethyl *N,N*-dimethylphosphoramidocyanidate; AcChE, human acetylcholinesterase; soman, *O*-pinacolyl methylphosphonofluoridate; cyclosarin, *O*-cyclohexyl methylphosphonofluoridate; 2-PAM, pralidoxime chloride; BuChE, human butyrylcholinesterase; hCE1, human carboxylesterase 1; DAM, 2,3-butanedione monoxime; r.m.s.d, root mean square deviation; pNPB, *para*-nitrophenyl butyrate; VX, *O*-ethyl *S*-(2-diisopropylaminoethyl) methylphosphonothioate.

Molecular Pharmacology Fast Forward. Published on January 5, 2010 as DOI: 10.1124/mol.109.062356
This article has not been copyedited and formatted. The final version may differ from this version.

ABSTRACT

Organophosphorus (OP) nerve agents are potent toxins that inhibit cholinesterases and produce a rapid and lethal cholinergic crisis. Development of protein-based therapeutics is being pursued with the goal of preventing nerve agent toxicity and protecting against the long-term side effects of these agents. The drug-metabolizing enzyme human carboxylesterase 1 (hCE1) is a candidate protein-based therapeutic due to its similarity in structure and function to the cholinesterase targets of nerve agent poisoning. However, the ability of wild-type hCE1 to process the G-type nerve agents sarin and cyclosarin has not been determined. We report the crystal structure of hCE1 in complex with the nerve agent cyclosarin. We further employ stereoselective nerve agent analogs to establish that hCE1 exhibits a 1,700- and 2,900-fold preference for the P_R enantiomers of analogs of soman and cyclosarin, respectively, and a 5-fold preference for the P_S isomer of a sarin analog. Finally, we show that for enzyme inhibited by racemic mixtures of *bona fide* nerve agents, hCE1 spontaneously reactivates in the presence of sarin but not soman or cyclosarin. Addition of the neutral oxime DAM increases the rate of reactivation of hCE1 from sarin inhibition by more than 60-fold, but has no effect on reactivation with the other agents examined. Taken together, these data demonstrate that hCE1 is only reactivated following inhibition with the more toxic P_S isomer of sarin. These results provide important insights toward the long-term goal of designing novel forms of hCE1 to act as protein-based therapeutics for nerve agent detoxification.

Molecular Pharmacology Fast Forward. Published on January 5, 2010 as DOI: 10.1124/mol.109.062356
This article has not been copyedited and formatted. The final version may differ from this version.

Originally discovered in 1854 as potent pesticides, organophosphorus (OP) nerve agents are some of the deadliest chemical compounds ever synthesized by humans (Newmark, 2007). During the Iran-Iraq war, Iranian soldiers were targeted with several chemical weapons, including sulfur mustard and the OP nerve agent sarin (*O*-isopropyl methylphosphonofluoridate). In 1988, Saddam Hussein used sarin and the related OP agent tabun (ethyl *N*,*N*-dimethylphosphoramidocyanidate) against Kurdish citizens in Halabja, killing 5,000 (Newmark, 2007). More recently, the cult Aum Shinrikyo released dilute sarin in the Tokyo system in 1995, killing 12 and affecting thousands (Okumura et al., 2005). Even though these and related compounds were banned by the 1997 Chemical Weapons Warfare Convention, their ease of synthesis and known use by rogue nations and terrorist groups continue to pose a security threat (Trapp, 2006).

OP nerve agents are alkylphosphonic esters **(Figure 1)** that covalently modify a variety of enzymes, most importantly the neurotransmitter regulating enzyme acetylcholinesterase (AcChE). AcChE inhibition leads to continual acetylcholine stimulus of the muscarinic and nicotinic receptors, resulting in seizures, convulsions, diaphragm incapacitation, and in cases of higher dose exposure, death. After phosphonylation of the catalytic serine in AcChE, a spontaneous, time-dependent dealkylation may occur (known as aging), resulting in a stable phosphonylated enzyme that is resistant to recovery therapies (Jokanovic, 2009). The P_S enantiomers of sarin, soman (*O*-pinacolyl methylphosphonofluoridate), and cyclosarin (*O*-cyclohexyl methylphosphonofluoridate) are significantly more lethal than the P_R isomers due to their preferential inhibition of the AcChE enzyme (Kovarik et al., 2003).

Current treatments for nerve agent poisoning include injections of atropine, a competitive inhibitor of acetylcholine at the muscarinic receptor, to turn off muscle stimulus, and a strong

Molecular Pharmacology Fast Forward. Published on January 5, 2010 as DOI: 10.1124/mol.109.062356
This article has not been copyedited and formatted. The final version may differ from this version.

nucleophilic oxime such as pralidoxime chloride (2-PAM), to dephosphonylate the AcChE catalytic serine prior to aging (Gray, 1984). Both of the compounds offer limited protection because they cannot be administered prior to exposure and do not address any of the long-term side effects associated with nerve agent poisoning (Doctor and Saxena, 2005). Prophylactic protein-based therapeutics are emerging as a means to protect against both toxicity and long-term side-effects in nerve agent poisoning (Lenz et al., 2007). These biological reagents act as "bioscavengers" to stoichiometrically sequester nerve agents prior to AcChE inhibition (Dunn and Sidell, 1989). Pre-administration of excess bioscavenger in mice provides protection against mortality equivalent to a post-exposure oxime injection, but is superior at minimizing post-exposure effects such as lacrimation or decreased motor function (Doctor and Saxena, 2005; Maxwell et al., 1993). Current stoichiometric bioscavengers include AcChE and the related serine hydrolase butyrylcholinesterase (BuChE). A more advanced protein-based therapeutic would include a catalytic function to detoxify nerve agents before AcChE inhibition reaches lethal levels. For example, human serum paraoxonase and bacterial organophosphorus hydrolase are being studied for this application (Lenz et al., 2007; Reeves et al., 2008).

Human carboxylesterase 1 (hCE1) is a 62 kDa serine hydrolase belonging to the same α/β hydrolase superfamily as AcChE and BuChE, but may offer some benefits over cholinesterases as a potential catalytic nerve agent hydrolase. Indeed, high serum carboxylesterase concentrations in rodents and mosquitoes protect these species from OP nerve agent exposure (Heidari et al., 2004; Maxwell, 1992). hCE1, found primarily in the liver, employs a catalytic triad composed of a serine, histidine and glutamic acid in a standard two-step serine hydrolase catalytic mechanism. hCE1 cleaves ester, thioester, and amine-ester bonds in a variety of endogenous and xenobiotic compounds (Redinbo and Potter, 2005). Previously, we

Molecular Pharmacology Fast Forward. Published on January 5, 2010 as DOI: 10.1124/mol.109.062356
This article has not been copyedited and formatted. The final version may differ from this version.

published the crystal structures of hCE1 in covalent acyl-enzyme complexes with the nerve agents soman and tabun (Fleming et al., 2007). However, the ability of hCE1 to reverse covalent inhibition and reactivate wild-type activity was not examined in that study.

Here we present a 3.1 Å X-ray non-aged crystal structure of hCE1 in covalent complex with the nerve agent cyclosarin, the first structure determined of any protein bound to this agent. To further examine the potential of hCE1 as either a bioscavenger or a nerve agent hydrolase, we utilized *bona fide* nerve agents and stereogenic analogs thereof to measure the bimolecular rates of inhibition, as well as the spontaneous and oxime-assisted rates of reactivation of hCE1 in the presence of sarin, soman, and cyclosarin. Lastly, we examine the propensity of hCE1 to age in the presence of nerve agent adducts. These crystallographic and biochemical data advance our understanding of the ability of hCE1 to process organophosphorus compounds, and will assist in the potential development of this enzyme as a protein-based therapeutic to prevent nerve agent toxicity.

MATERIALS AND METHODS

Nerve Agent Inhibition and Crystallization. hCE1 was expressed and secreted from baculovirus-infected *Spodoptera frugiperda* Sf21 cells, and purified to >98% homogeneity by SDS-PAGE as previously described (Morton and Potter, 2000). At USAMRICD, two milligrams of purified protein were incubated with ~10-fold molar excess of racemic cyclosarin (obtained from the Research Development and Engineering Command, Aberdeen Proving Ground, MD) for 1 hour at room temperature. Excess unbound agent was removed by passing inhibited hCE1 over a PD-10 Sephadex G-25 size exclusion chromatography column (Amersham Biosciences, Uppsala, Sweden). Post-column samples were tested to confirm

Molecular Pharmacology Fast Forward. Published on January 5, 2010 as DOI: 10.1124/mol.109.062356
This article has not been copyedited and formatted. The final version may differ from this version.

complete inhibition by measuring hydrolysis of *para*-nitrophenyl butyrate (pNPB, Sigma), a conventional esterase substrate (Wierdl et al., 2008). To assess the extent to which excess cyclosarin was retained within the column, the capacity of the eluate to subsequently inhibit BuChE was also determined. Cyclosarin inhibited hCE1 was concentrated to 3 mg/mL using Amicon Ultra-15 (Millipore) spin concentrators. Plate-like crystals (600 µM x 100 µM x 50 µM) were grown in 4-6 weeks using the sitting drop vapor-diffusion method in 10% PEG 3350, 0.3 M Li_2SO_4, 0.1 M Citrate pH 5.5, 0.1 M NaCl, 0.1 M LiCl, and 5% glycerol. Prior to cooling to 100 K in liquid nitrogen, crystals were cryoprotected by stepwise passages into a final concentration of 30% (w/v) sucrose plus mother liquor.

Structure Determination and Refinement. X-Ray diffraction data were collected at 100 K at the Advanced Photon Source at Argonne National Laboratory (Argonne, IL) on beam line 22-ID (SER-CAT). Data were indexed and scaled using the XDS package (Kabsch, 1988). Molecular replacement was conducted using MolRep in the CCP4i suite (Collaborative Computation Project, 1994) (v. 6.1.0) with one trimer of the hCE1-tacrine structure (RSCB PDB accession code 1MX1 (Bencharit et al., 2003)) as the search model. The hCE1-cyclosarin model was refined using rigid body, simulated annealing, and grouped *B*-factor refinements in CNS (Brunger et al., 1998) that included an overall anisotropic *B*-factor, bulk solvent correction, and non-crystallographic symmetry (NCS) restraints for regions outside the active site. Prior to any structural refinement, a subset (7%) of the data was set aside for cross-validation by R_{free} calculation. Manual building was conducted in Coot (Emsley and Cowtan, 2004) with σ_a-weighted composite omit, difference density, and simulated annealing omit maps. Data collection and refinement statistics were summarized and are presented in **Table 1**. The final structure was validated using PROCHECK (Laskowski et al., 1993), and all figures were

Molecular Pharmacology Fast Forward. Published on January 5, 2010 as DOI: 10.1124/mol.109.062356
This article has not been copyedited and formatted. The final version may differ from this version.

generated in PyMol (DeLano Scientific, Palo Alto, CA). Coordinates and structure factors have been deposited at the PDB with accession code 3K9B.

Inhibition Rate Constants using Nerve Agent Analogues. Samples of purified hCE1 at 100 nM were inhibited at room temperature with increasing concentrations of stereogenic OP nerve agent analogs. Aliquots of enzyme incubated with stereoisomer analogs of sarin (P_R, P_S), P_S soman, and P_S cyclosarin were removed at various time points (up to 1 hr) and the level of active enzyme that remained was determined by comparing pNPB hydrolysis relative to an uninhibited sample. Because the P_R soman and P_R cyclosarin analogs react more quickly with hCE1, the impacts these analogs had on hCE1 were measured continuously (for up to 15 min) by adding increasing concentrations of analog to hCE1 samples containing pNPB and measuring loss of functional enzyme activity over time. These data, collected at 410 nm and 25 ^{o}C on a Pherastar microplate reader (BMG Labtech), were corrected for spontaneous pNPB hydrolysis and fit to equation 1 (Aurbek et al., 2006):

$$\frac{\Delta t}{\Delta \ln v} = \frac{K_{\mathrm{d}}}{k_2} * \frac{1}{[\mathrm{IX}](1-\alpha)} + \frac{1}{k_2} \qquad (1)$$

where K_{d} was the dissociation constant, k_2 the unimolecular phosphorylation rate constant, v the remaining percent enzyme activity, [IX] was the OP analog concentration, α was $[S]/(K_{\mathrm{M}}+[S])$, in which [S] was the substrate concentration and K_{M} was the Michaelis-Menton constant. All experiments were performed in triplicate. Data were analyzed in KaleidaGraph 4 (Synergy Software, Reading, PA) to determine k_{i} ($k_{\mathrm{i}} = k_2 / K_{\mathrm{d}}$) values.

Spontaneous Reactivation. Fifty µL of COS cell lysate expressing a non-secreted form of hCE1, prepared as previously described (Wierdl et al., 2008), was inhibited with a ~1000- fold molar excess of racemic OP agents sarin, soman, or cyclosarin for 10 min. Excess agent was removed by passing inhibited samples over a PD-10 Sephadex G-25 size exclusion column. The

Molecular Pharmacology Fast Forward. Published on January 5, 2010 as DOI: 10.1124/mol.109.062356
This article has not been copyedited and formatted. The final version may differ from this version.

column eluate was diluted 10-fold in 0.1 M potassium phosphate buffer, pH 7.4 and tested for the presence or absence of CE activity and complete removal of excess agent, as previously described. Aliquots were removed over time (up to 80 hrs) and the percent enzyme activity was measured by pNPB hydrolysis relative to an uninhibited sample. The rate of reactivation (k_{obs}) and maximal percent recovery (A_{max}) were determined by fitting the data to equation 2:

$$A = A_0 + A_{max}(1 - e^{-k_{obs}t}) \quad (2)$$

where A was percent activity at time, t, and A_0 was initial activity at t=0. The experiments were conducted in triplicate and data were analyzed with Sigma Plot v.8.02 (Systat, Chicago, IL).

Oxime-Assisted Reactivation. Fifty µL of COS cell lysate containing hCE1 were inhibited and excess agent was removed as previously described. Stereogenic OP analogs were utilized in a similar fashion to racemic nerve agents, but required a longer incubation time (up to 1 hr). Upon column elution, samples were diluted 10-fold into 1 mM 2,3-butanedione monoxime (DAM, Sigma), which had been previously prepared in 0.1 M potassium phosphate pH 7.4 and kept on ice. DAM had no inhibitory effect on hCE1 at this concentration (data not shown). Aliquots were removed over time and enzyme activity was measured as described above. The rate of reactivation (k_{obs}) and maximal percent reactivation (A_{max}) were determined for each agent/analog by subtracting background oxime-induced pNPB hydrolysis and fitting the data to equation 2.

Aging. Samples of 1 µM purified hCE1 were inhibited with a 1,000-fold molar excess of the P_S sarin, soman, and cyclosarin analogs for 60 minutes at room temperature. Complete inhibition was verified by the absence of pNPB hydrolysis. Excess unbound agent was removed by size exclusion chromatography as previously described, and aliquots were diluted 1:10 into 1 mM DAM every 12 hours for 48 hours. After dilution into DAM, each sample was incubated for 24

Molecular Pharmacology Fast Forward. Published on January 5, 2010 as DOI: 10.1124/mol.109.062356
This article has not been copyedited and formatted. The final version may differ from this version.

hours to achieve maximal DAM-assisted reactivation, and then enzyme activity was measured and percent reactivation was determined relative to an uninhibited sample. Maximum percent reactivation (A_{max}) was plotted against the incubation time in the absence of DAM and fit to equation 3 (Shafferman et al., 1996):

$$A_{max} = A_{max0} \exp^{-k_a t} \quad (3)$$

where A_{max0} was the maximum recovery at time=0, and k_a was the rate of aging.

RESULTS

Crystal Structure of the hCE1-Cyclosarin Complex. The crystal structure of hCE1 in a covalent acyl-enzyme intermediate complex with the OP nerve agent cyclosarin was determined by molecular replacement and refined to 3.1 Å resolution (**Table 1**). The hCE1-cyclosarin structure was similar to ligand complexes of this enzyme described previously, with a root-mean-square deviation (r.m.s.d.) of 0.48 Å over 1,354 equivalent Cα positions when compared to the hCE1-tacrine structure (Bencharit et al., 2003). The initial maps were of good quality for the majority of the polypeptide, with the exception of the acyl-loop (residues 304-318) that caps the active site and five short loops (340-342, 369-374, 406-410, 450-454, 483-488) between secondary structural elements. When positioned provisionally, these disordered regions displayed *B*-factors of >90 Å^2; in contrast, the average *B*-factor of the ordered regions of the final model was 54 Å^2. Two of these regions (369-374, 450-454) were also disordered in the structure of a rabbit liver carboxylesterase, which shares 81 % sequence identity and 0.42 Å r.m.s.d. over 401 equivalent Cα positions relative to hCE1 (Bencharit et al., 2002). The model of hCE1 complexed with cyclosarin was refined to final *R* factors of 26.6% (R_{cryst}) and 29.9% (R_{free}) **(Table 1)**.

Molecular Pharmacology Fast Forward. Published on January 5, 2010 as DOI: 10.1124/mol.109.062356
This article has not been copyedited and formatted. The final version may differ from this version.

Each hCE1 monomer, supported by two disulfide links (Cys87-Cys116, Cys274-Cys285), contained two ligand binding sites within three domains: catalytic, α/β, and regulatory (Bencharit et al., 2002) **(Figure 2)**. The hCE1-trimer was formed through C3 symmetry around respective α/β domains and buries 475 $Å^2$ of solvent-accessible surface area per protein monomer. The primary ligand binding site, the active site, was located at the interface of the three domains in each monomer, and was composed of the Ser221, His468, and Glu354 catalytic triad. The second ligand binding site (or Z-site) was on the enzyme's surface at the interface between the regulatory and catalytic domains. Previous crystal structures of hCE1 in complex with OP nerve agents soman and tabun contained sucrose, the cryoprotectant, in the Z-site (Fleming et al., 2007). Ser 369, which forms a hydrogen bond with the O1 of sucrose in these other structures, was disordered in the hCE1-cyclosarin structure and no ligand molecule was observed in this site. The catalytic domain also contained a high-mannose glycosylation site at Asn79. Density was observed around Asn79 but neither *N*-acetylglucosamine nor terminal sialic acid could be reliably built and refined into this region.

OP nerve agents inhibit hCE1 by forming a covalent adduct with the catalytic serine **(Figure 3A)**. In the structure of the hCE1-cyclosarin complex reported here, a covalent cyclosarin adduct was easily identified in initial difference density ($F_0 - F_c$) maps as a 6 σ electron density peak approximately 1.6 Å away from the Ser 221 Oγ, which corresponded to the nerve agent phosphate. At lower σ levels (2.5-4 σ), additional density for the complete molecule was apparent. The cyclosarin model was built into the observed density, refined, and P_R stereochemistry was assigned around the chiral phosphate **(Figure 3B)**. The acyl-enzyme adduct was stabilized by two hydrogen bonds. These occur between the cyclosarin phosphoryl oxygen atom and hydrogen atoms present on the amide nitrogens within residues Gly142 and Gly143

Molecular Pharmacology Fast Forward. Published on January 5, 2010 as DOI: 10.1124/mol.109.062356
This article has not been copyedited and formatted. The final version may differ from this version.

(2.6 Å and 2.4 Å, respectively). The *O*-cyclohexyl alkoxy group is located within in the larger, flexible pocket of the active site and is stabilized by interactions with Leu363 of the regulatory domain. The stereochemistry and alkoxy placement was confirmed with a 3.1 Å resolution simulated annealing omit map, contoured to 5 σ **(Figure 4A)**. The opposite P_S isomer was also built into the starting model and one round of refinement was performed. Clear positive and negative density from a difference density map ($|F_0 - F_c|, \phi_{calc}$) verified the P_R assignment as consistent with the biochemical results **(Figure 4B)**.

Nerve Agent Analog Stereopreference of hCE1. Sarin, soman, and cyclosarin contain a chiral phosphorus atom and exist as racemic mixtures of P_R and P_S stereoisomers. Soman also has an asymmetric carbon (Cα) in the pinacolyl group. The P_S isomers of sarin, soman and cyclosarin inhibit AcChE more potently than the P_R forms; for example, the preference of P_S vs. P_R soman is 5,000-fold for AcChE (Sanson et al., 2009). Using OP nerve agent analogs containing a thiomethyl-leaving group prepared as purified stereoisomers (**Figure 1**), we determined the stereoselectivity of hCE1 inhibition by analogs of sarin, soman, and cyclosarin **(Figure 5)**. These analogs have been shown by MALDI-TOF mass spectrometry to yield, among other products, acyl-enzyme adducts identical to those from authentic agents when used to inhibit butyrylcholinesterase (Gilley et al., 2009). The thiomethyl-leaving group that replaces the fluoride atom found in nerve agents decreases the toxicity of the analogs by slowing the rate of phosphonylation (k_2) compared to real agents; however, the dissociation constants (K_d) remain similar (Forsberg and Puu, 1984). The decrease in k_2 results in a reduction in the bimolecular rate of inhibition (k_i) by 2-3 orders of magnitude when compared to the corresponding nerve agent (Maxwell, 1992). P_R analogs of soman and cyclosarin inhibited hCE1 1,700- and 2,900-fold more efficiently than the P_S isomers, respectively (**Figure 5**). In contrast, hCE1 exhibited a

Molecular Pharmacology Fast Forward. Published on January 5, 2010 as DOI: 10.1124/mol.109.062356
This article has not been copyedited and formatted. The final version may differ from this version.

5-fold preference for the P_S vs. P_R form of the sarin analogs (**Figure 5**). As discussed below, this may be because the smaller *O*-isopropyl group in the sarin analogs is more easily accommodated in the hCE1 active site than that larger *O*-pinacolyl and *O*-cyclohexyl groups of the soman and cyclosarin analogs, respectively. Taken together, these results demonstrate that hCE1 exhibites a strong preference for the P_R soman and cyclosarin analogs, and a smaller preference for the P_S isomer of the smaller, sarin analog.

Spontaneous Reactivation of hCE1. After the formation of the acyl-enzyme intermediate, proteins exposed to OP nerve agents may remain stably adducted, permanently inhibited (aged), or undergo spontaneous hydrolysis (hereafter referred to as reactivation) reversing the phosphonylation and returning the enzyme to normal function (Langenberg et al., 1988; Li et al., 2007). To test the ability of hCE1 to reactivate after inhibition by nerve agents, the enzyme was challenged with racemic mixtures of the OP nerve agents soman, sarin, and cyclosarin. We found that only samples inhibited with sarin exhibited spontaneous reactivation **(Figure 6A)**, with a half-time of 45 hours (k_{obs}=2.58 ± 0.06 x 10^{-4} min^{-1}). When carried out to 300 hours, a maximum activity of 84 ± 6% was recovered (data not shown). The rate of reactivation was approximately 10-fold slower than that measured for rat serum carboxylesterase (Maxwell and Brecht, 2001), but 10-fold faster than BuChE (Bartling et al., 2007). In contrast, AcChE exhibits no reactivation following sarin inhibition (Bartling et al., 2007). hCE1 inhibited with soman and cyclosarin, however, exhibited poor reactivation and achieved a maximum recovery of activity of only ~10% even after 300 hours (**Figure 6A**). These data establish that reactivation of hCE1 only occurs following exposure to sarin.

Oxime-Assisted Reactivation of hCE1. Strong oxime nucleophiles like 2-PAM and obidoxime are known to reactivate OP-inhibited esterases, particularly AcChE, by promoting the

Molecular Pharmacology Fast Forward. Published on January 5, 2010 as DOI: 10.1124/mol.109.062356
This article has not been copyedited and formatted. The final version may differ from this version.

dephosphonylation of the active site serine. These cationic oximes are currently used as part of post-exposure therapy and are appropriate for the anionic choline binding gorge in cholinesterases (Volans, 1996). Carboxylesterases such as hCE1 react poorly with charged substrates (Maxwell et al., 1994); however, the ability of a neutral oxime like DAM to reactivate inhibited hCE1 had not been reported in the literature. Thus, we tested whether DAM would reactivate hCE1 that had been exposed to racemic mixtures of OP nerve agents. We found that DAM enhanced the reactivation of sarin-inhibited hCE1, but not enzyme inhibited by soman or cyclosarin **(Figure 6B)**. In the presence of DAM, sarin-inhibited hCE1 exhibited a half-time of reactivation of 41 minutes (k_{obs}=0.0168 ± 0.0003 min^{-1} mM^{-1}), approximately 66-fold faster than that observed without the oxime (see **Figure 6A**). In addition, similar to spontaneous reactivation, the maximal recovery of hCE1 that was observed in the presence of DAM was 89 ± 4%. Thus, the neutral oxime DAM increased the rate of reactivation of sarin-inhibited hCE1 by more than 65-fold.

We next examined the ability of DAM to enhance the reactivation of hCE1 inhibited with pure enantiomeric P_R or P_S isoforms of the nerve agent analogs (see **Figure 1**). We found that hCE1 inhibited with the P_S sarin analog exhibited reactivation with a half-time of 30 minutes (k_{obs}=0.023 ± 0.004 min^{-1} mM^{-1}), while hCE1 inhibited by the P_R sarin analog exhibited no detectable reactivation (**Figure 6C**). In contrast, hCE1 samples inhibited with P_S soman and cyclosarin analogs were capable of marginal reactivation, while respective P_R analogs displayed no recovery **(Figures 6D, 6E)**. Taken together, these data suggest that the reactivation of hCE1 in the presence of the sarin analog was due to the hydrolysis of the P_S isomer, while the P_R isomer cannot be removed from the active site even in the presence of DAM.

Molecular Pharmacology Fast Forward. Published on January 5, 2010 as DOI: 10.1124/mol.109.062356
This article has not been copyedited and formatted. The final version may differ from this version.

Aging in OP-inhibited hCE1. Aging in serine hydrolases involves the time-dependent dealkylation of the bound adduct, resulting in a permanently phosphorylated catalytic serine residue (Li et al., 2007). This process is rapid for soman in the active site of AcChE ($t_{1/2}$ of ~2 minutes), and is the primary cause of the toxicity of this agent (Sanson et al., 2009). Once aging has occurred, nerve agent adducts are inert even to strong oximes. We explored the propensity of hCE1 to age in the presence of nerve agent analog P_S stereoisomers by measuring the loss in the maximal level of DAM-mediated reactivation (A_{max}) over time. If the nerve agent analog adduct undergoes time-dependent dealkylation, one would expect an exponential decay for A_{max} (Shafferman et al., 1996). Over 48 hours, no change in A_{max} was observed for any of the agent analogs **(Figure 6F)**. For example, after two hours exposure of hCE1 to the P_S sarin analog, DAM was capable of reactivating ~60% of the enzyme activity (see **Figure 6B**); however, even after 46 additional hours of incubation with this sarin analog, the same fraction of enzyme activity, recovered by DAM, was observed (see **Figure 6F**). Thus, sarin-inhibited hCE1 does not appear to undergo the same first-order aging process that has been observed with other serine hydrolases, such as AcChE.

DISCUSSION

Organophosphorus nerve agents inactivate the neurotransmitter-regulating enzyme acetylcholinesterase and bind to other physiologically important proteins, such as albumin, lipases, and carboxylesterases (Fleming et al., 2007; Li et al., 2008). As such, these toxins are among the deadliest compounds developed by humans. The U.S. military has pursued the development of enzyme therapies capable of protecting personnel from nerve agent exposure (Lenz et al., 2007). Accordingly, in this report, we present X-ray crystallographic and

Molecular Pharmacology Fast Forward. Published on January 5, 2010 as DOI: 10.1124/mol.109.062356
This article has not been copyedited and formatted. The final version may differ from this version.

biochemical data designed to evaluate the ability of human carboxylesterase 1 (hCE1) to act as potential enzyme-based therapeutic for nerve agent detoxification. While we have previously determined crystal structures of hCE1 in complexes with soman and tabun (Fleming et al., 2007), here we report the novel crystal structure of hCE1 inhibited by cyclosarin **(Figure 2)**, one of the most potent inhibitors of human AcChE (Gray and Dawson, 1987). Difference density and simulated annealing omit maps facilitated the placement of a covalent adduct with P_R stereochemistry bound to the catalytic Ser-221 of hCE1 **(Figure 3A)**. After covalent adduction of OP nerve agents and analogs to the catalytic serine, stereochemistry at the phosphorus atom remains the same. A rearrangement in priority assignment after collapse of the pentahedral intermediate causes the covalent phosphonyl-enzyme intermediate to retain the original stereochemistry of the OP compound prior to enzyme binding (Epstein et al., 2009). Therefore, the P_R stereochemistry observed in the crystal structure of the hCE1-cyclosarin acyl-enzyme adduct (see **Figures 3-4**) corresponds to the preferential reaction of hCE1 with the P_R analog of cyclosarin.

Indeed, using thiomethyl-substituted nerve agent analogs, we were able to complete experiments designed to examine the stereoselectivity of hCE1 for these analogs of sarin, soman, and cyclosarin **(Figure 4)**. We found that hCE1 preferentially binds to the P_R isomers of cyclosarin and soman analogs, which is opposite to the stereopreference observed for AcChE with *bona fide* nerve agents. A structural comparison of the hCE1-soman and hCE1-cyclosarin crystal structures with AcChE-soman (RSCB PDB code 2WGO (Sanson et al., 2009)) reveals that the bulky P_R *O*-alkoxy group is positioned into the larger hydrophobic binding pocket of hCE1. In contrast, this region is occupied in AcChE by a long acyl loop that dips into the active site pocket and precludes binding of P_R nerve agents (Fleming et al., 2007; Sanson et al., 2009).

Molecular Pharmacology Fast Forward. Published on January 5, 2010 as DOI: 10.1124/mol.109.062356
This article has not been copyedited and formatted. The final version may differ from this version.

Therefore, the geometry of the hCE1 active site size dictates the enantiomeric binding of the bulkier nerve agents soman and cyclosarin. With the smaller nerve agent sarin, hCE1 demonstrated only a 5-fold preference for the P_S isomer of the sarin nerve agent analog **(Figure 5)**. Our structures indicate that while both isomers of sarin will fit in the active site of the enzyme, only P_S sarin is capable of forming stabilizing hydrophobic contacts with Phe101 and Leu97; P_R sarin would not form analogous interactions **(Figure 7A)**. These structural considerations, in part, explain the observed strong preference for P_R soman and cyclosarin, and the relatively weak preference for P_S sarin exhibited by hCE1.

Following the formation of the acyl-enzyme intermediate, the first step of the serine hydrolase catalytic mechanism (see **Figure 3A**), nerve agent-esterase complexes can undergo reactivation or aging. Both spontaneous and oxime-assisted reactivation displaces the acyl-enzyme intermediate and restores the enzyme to normal function. We found that nerve agent-inhibited hCE1 only reactivates spontaneously, or with the oxime DAM, following incubation with sarin (**Figures 6A, 6B**). In addition, while DAM enhanced the rate of reactivation 66-fold, both spontaneous and oxime-assisted reactivation only restores ~85% of the original enzyme activity. Utilizing the stereogenic nerve agent analogs we showed that the rate of DAM-assisted reactivation following inhibition with the P_S sarin analog was identical, within error, to the rate of DAM-assisted reactivation for racemic sarin (**Figures 6B, 6C**). No recovery was measured for the P_R sarin analog (**Figure 6C**). In contrast to sarin, hCE1 incubated with racemic samples of the nerve agents soman or cyclosarin exhibited relatively little reactivation (**Figures 6A, 6B**). Furthermore, only weak reactivation was only achieved with the P_S isomers when analogs of these nerve agents were incubated with hCE1 (**Figures 6D, 6E**). Based on these data, we conclude that hCE1 stereoselectively reactivates P_S sarin following racemic inhibition.

Molecular Pharmacology Fast Forward. Published on January 5, 2010 as DOI: 10.1124/mol.109.062356
This article has not been copyedited and formatted. The final version may differ from this version.

We next modeled how hCE1 might preferentially reactivate in the presence of P_S sarin (**Figure 7B**). Previous work investigating the influence of pH on spontaneous reactivation in AcChE identified the importance of two ionizable residues with pKa values of 6.9 and 9.8, suggesting possible His and Tyr residues, respectively (Reiner and Aldridge, 1967). In the hCE1 active site, the catalytic His468 neighbors P_S sarin and Tyr152 is located approximately 8 Å away. These two residues are connected via a hydrogen-bonding network through Glu200 (**Figure 7B**). It has been observed in the structure of the AcChE covalent complex with non-aged P_S VX that the protonated Nε2 of His440 (H468 in hCE1) rotates away from Ser200 (Ser221 in hCE1) to form a hydrogen-bond with Glu199 (Glu220 in hCE1) (Millard et al., 1999). The Nε2 movement would be expected to be blocked in hCE1 by larger alkoxy groups, such as the *O*-pinacolyl group in soman, and is not observed in the non-aged AcChE soman structure (Sanson et al., 2009). If this shift occurs in hCE1 with P_S sarin, however, the His468 Nε2 rotation to Glu220 would reorient the remaining His468 nitrogen, Nδ1, formerly hydrogen-bonded to Glu354. It would then be positioned to interact with the P_S sarin O2 atom and may act as a general base for hydrolytic dephosphonylation (**Figure 7B**). An analogous orientation of the O2 atom of P_R sarin would not be possible while still maintaining interactions with the oxyanion hole (see **Figure 7A**). By this model, hCE1 will only reactivate after inhibition with P_S sarin, consistent with the experimental results presented above. However, the rate of reactivation is observed to be poor, likely due to the weak nucleophilicity of Tyr152 at pH 7.4.

Organophosphinate-esterase complexes may also undergo aging. While P_S isomers of OPs showed some capability to be removed from the hCE1 active site by reactivation (see **Figure 6C, 6D, 6E**), we saw no evidence for first-order aging in hCE1 (**Figure 6F**). We therefore considered what the fate of the P_R-hCE1 adducts are if they do not age, and the state of

Molecular Pharmacology Fast Forward. Published on January 5, 2010 as DOI: 10.1124/mol.109.062356
This article has not been copyedited and formatted. The final version may differ from this version.

the remaining percent of P_S-hCE1 adducts that do not undergo reactivation. For complexes of P_R organophosphates and hCE1, we propose that they remain at the acyl-enzyme intermediate stage of the enzyme's reaction mechanism. This state has been observed in the hCE1-P_R soman and hCE1-P_R cyclosarin crystal structures, and via MALDI-TOF analysis of BuChE inhibited by P_R analogs of sarin, soman, and cyclosarin (Gilley et al., 2009). For the 40% of P_S-sarin analog complexes with hCE1 that do not undergo reactivation, we propose that an alternate Ser221 state is created. In addition to forming adducts identical to authentic agents, the thiomethyl-nerve agent analogs utilized in this study have been shown to undergo a unique reaction, where the *O*-alkoxy rather than the thiomethyl group is displaced upon collapse of the original pentahedral intermediate (Gilley et al., 2009). Therefore, dehydroalanine formation at the catalytic serine might also occur with these nerve agent analogs. Mass spectrometry studies were attempted to confirm or deny the presence of this adduct in hCE1; unfortunately, the peptide fragment containing Ser221 could not be isolated and no useful data were obtained (personal communication with Dr. Oksana Lockridge).

In summary, these studies establish the stereopreference of wild-type hCE1 for nerve agent analogs of cyclosarin, soman and sarin, and confirm this preference for cyclosarin with crystallographic data. In addition, they indicate that the native form of hCE1 is capable of reactivation after incubation with the nerve agent sarin, and that the rate of reactivation is enhanced with the neutral oxime DAM. In future studies, we will use these data to design mutant forms of hCE1 with the goal of enhancing nerve agent hydrolysis for not only sarin, but also soman and cyclosarin.

Molecular Pharmacology Fast Forward. Published on January 5, 2010 as DOI: 10.1124/mol.109.062356
This article has not been copyedited and formatted. The final version may differ from this version.

ACKNOWLEDGEMENTS

The authors thank the Redinbo Lab, particularly Dr. Sarah Kennedy and Rebekah Nash, for assistance in x-ray data collection and manuscript preparation.

REFERENCES

Aurbek N, Thiermann H, Szinicz L, Eyer P and Worek F (2006) Analysis of inhibition, reactivation and aging kinetics of highly toxic organophosphorus compounds with human and pig acetylcholinesterase. *Toxicology* **224**(1-2):91-99.

Bartling A, Worek F, Szinicz L and Thiermann H (2007) Enzyme-kinetic investigation of different sarin analogues reacting with human acetylcholinesterase and butyrylcholinesterase. *Toxicology* **233**(1-3):166-172.

Bencharit S, Morton CL, Howard-Williams EL, Danks MK, Potter PM and Redinbo MR (2002) Structural insights into CPT-11 activation by mammalian carboxylesterases. *Nat Struct Biol* **9**(5):337-342.

Bencharit S, Morton CL, Hyatt JL, Kuhn P, Danks MK, Potter PM and Redinbo MR (2003) Crystal structure of human carboxylesterase 1 complexed with the Alzheimer's drug tacrine: from binding promiscuity to selective inhibition. *Chem Biol* **10**(4):341-349.

Brunger AT, Adams PD, Clore GM, DeLano WL, Gros P, Grosse-Kunstleve RW, Jiang JS, Kuszewski J, Nilges M, Pannu NS, Read RJ, Rice LM, Simonson T and Warren GL (1998) Crystallography & NMR system: A new software suite for macromolecular structure determination. *Acta Crystallogr D Biol Crystallogr* **54**(Pt 5):905-921.

Collaborative Computation Project N (1994) The CCP4i suite: programs for protein crystallography. *Acta Crystallogr D Biol Crystallogr* **50**(760-763).

Doctor BP and Saxena A (2005) Bioscavengers for the protection of humans against organophosphate toxicity. *Chem Biol Interact* **157-158**:167-171.

Dunn MA and Sidell FR (1989) Progress in medical defense against nerve agents. *Jama* **262**(5):649-652.

Emsley P and Cowtan K (2004) Coot: model-building tools for molecular graphics. *Acta Crystallogr D Biol Crystallogr* **60**(Pt 12 Pt 1):2126-2132.

Epstein TM, Samanta U, Kirby SD, Cerasoli DM and Bahnson BJ (2009) Crystal structures of brain group-VIII phospholipase A2 in nonaged complexes with the organophosphorus nerve agents soman and sarin. *Biochemistry* **48**(15):3425-3435.

Fleming CD, Edwards CC, Kirby SD, Maxwell DM, Potter PM, Cerasoli DM and Redinbo MR (2007) Crystal structures of human carboxylesterase 1 in covalent complexes with the chemical warfare agents soman and tabun. *Biochemistry* **46**(17):5063-5071.

Forsberg A and Puu G (1984) Kinetics for the inhibition of acetylcholinesterase from the electric eel by some organophosphates and carbamates. *Eur J Biochem* **140**(1):153-156.

Gilley C, MacDonald M, Nachon F, Schopfer LM, Zhang J, Cashman JR and Lockridge O (2009) Nerve agent analogues that produce authentic soman, sarin, tabun, and cyclohexyl methylphosphonate-modified human butyrylcholinesterase. *Chem Res Toxicol* **22**(10):1680-1688.

Gray AP (1984) Design and structure-activity relationships of antidotes to organophosphorus anticholinesterase agents. *Drug Metab Rev* **15**(3):557-589.

Gray PJ and Dawson RM (1987) Kinetic constants for the inhibition of eel and rabbit brain acetylcholinesterase by some organophosphates and carbamates of military significance. *Toxicol Appl Pharmacol* **91**(1):140-144.

Heidari R, Devonshire AL, Campbell BE, Bell KL, Dorrian SJ, Oakeshott JG and Russell RJ (2004) Hydrolysis of organophosphorus insecticides by in vitro modified carboxylesterase E3 from Lucilia cuprina. *Insect Biochem Mol Biol* **34**(4):353-363.

Jokanovic M (2009) Current understanding of the mechanisms involved in metabolic detoxification of warfare nerve agents. *Toxicol Lett* **188**(1):1-10.

Kabsch W (1988) Evaluation of single-crystal X-ray diffraction data from a position-sensitive detector. *J Appl Cryst* **21**:916-924.

Kovarik Z, Radic Z, Berman HA, Simeon-Rudolf V, Reiner E and Taylor P (2003) Acetylcholinesterase active centre and gorge conformations analysed by combinatorial mutations and enantiomeric phosphonates. *Biochem J* **373**(Pt 1):33-40.

Langenberg JP, De Jong LP, Otto MF and Benschop HP (1988) Spontaneous and oxime-induced reactivation of acetylcholinesterase inhibited by phosphoramidates. *Arch Toxicol* **62**(4):305-310.

Laskowski R, MacArthur M, Moss D and Thornton J (1993) PROCHECK: a program to check the stereochemical quality of protein structures. *J Appl Cryst* **26**:283-291.

Lenz DE, Yeung D, Smith JR, Sweeney RE, Lumley LA and Cerasoli DM (2007) Stoichiometric and catalytic scavengers as protection against nerve agent toxicity: a mini review. *Toxicology* **233**(1-3):31-39.

Li B, Nachon F, Froment MT, Verdier L, Debouzy JC, Brasme B, Gillon E, Schopfer LM, Lockridge O and Masson P (2008) Binding and hydrolysis of soman by human serum albumin. *Chem Res Toxicol* **21**(2):421-431.

Li H, Schopfer LM, Nachon F, Froment MT, Masson P and Lockridge O (2007) Aging pathways for organophosphate-inhibited human butyrylcholinesterase, including novel pathways for isomalathion, resolved by mass spectrometry. *Toxicol Sci* **100**(1):136-145.

Maxwell DM (1992) The specificity of carboxylesterase protection against the toxicity of organophosphorus compounds. *Toxicol Appl Pharmacol* **114**(2):306-312.

Maxwell DM and Brecht KM (2001) Carboxylesterase: specificity and spontaneous reactivation of an endogenous scavenger for organophosphorus compounds. *J Appl Toxicol* **21 Suppl 1**:S103-107.

Maxwell DM, Brecht KM, Doctor BP and Wolfe AD (1993) Comparison of antidote protection against soman by pyridostigmine, HI-6 and acetylcholinesterase. *J Pharmacol Exp Ther* **264**(3):1085-1089.

Maxwell DM, Lieske CN and Brecht KM (1994) Oxime-induced reactivation of carboxylesterase inhibited by organophosphorus compounds. *Chem Res Toxicol* **7**(3):428-433.

Millard CB, Kryger G, Ordentlich A, Greenblatt HM, Harel M, Raves ML, Segall Y, Barak D, Shafferman A, Silman I and Sussman JL (1999) Crystal structures of aged phosphonylated acetylcholinesterase: nerve agent reaction products at the atomic level. *Biochemistry* **38**(22):7032-7039.

Morton CL and Potter PM (2000) Comparison of Escherichia coli, Saccharomyces cerevisiae, Pichia pastoris, Spodoptera frugiperda, and COS7 cells for recombinant gene expression. Application to a rabbit liver carboxylesterase. *Mol Biotechnol* **16**(3):193-202.

Newmark J (2007) Nerve agents. *Neurologist* **13**(1):20-32.

Okumura T, Hisaoka T, Yamada A, Naito T, Isonuma H, Okumura S, Miura K, Sakurada M, Maekawa H, Ishimatsu S, Takasu N and Suzuki K (2005) The Tokyo subway sarin attack--lessons learned. *Toxicol Appl Pharmacol* **207**(2 Suppl):471-476.

Redinbo MR and Potter PM (2005) Mammalian carboxylesterases: from drug targets to protein therapeutics. *Drug Discov Today* **10**(5):313-325.

Reeves TE, Wales ME, Grimsley JK, Li P, Cerasoli DM and Wild JR (2008) Balancing the stability and the catalytic specificities of OP hydrolases with enhanced V-agent activities. *Protein Eng Des Sel* **21**(6):405-412.

Reiner E and Aldridge WN (1967) Effect of pH on inhibition and spontaneous reactivation of acetylcholinesterase treated with esters of phosphorus acids and of carbamic acids. *Biochem J* **105**(1):171-179.

Sanson B, Nachon F, Colletier JP, Froment MT, Toker L, Greenblatt HM, Sussman JL, Ashani Y, Masson P, Silman I and Weik M (2009) Crystallographic Snapshots of Nonaged and Aged Conjugates of Soman with Acetylcholinesterase, and of a Ternary Complex of the Aged Conjugate with Pralidoxime (dagger). *J Med Chem*.

Shafferman A, Ordentlich A, Barak D, Stein D, Ariel N and Velan B (1996) Aging of phosphylated human acetylcholinesterase: catalytic processes mediated by aromatic and polar residues of the active centre. *Biochem J* **318 (Pt 3)**:833-840.

Trapp R (2006) Worldwide governmental efforts to locate and destroy chemical weapons and weapons materials: minimizing risk in transport and destruction. *Ann N Y Acad Sci* **1076**:527-539.

Volans AP (1996) Sarin: guidelines on the management of victims of a nerve gas attack. *J Accid Emerg Med* **13**(3):202-206.

Wierdl M, Tsurkan L, Hyatt JL, Edwards CC, Hatfield MJ, Morton CL, Houghton PJ, Danks MK, Redinbo MR and Potter PM (2008) An improved human carboxylesterase for enzyme/prodrug therapy with CPT-11. *Cancer Gene Ther* **15**(3):183-192.

Molecular Pharmacology Fast Forward. Published on January 5, 2010 as DOI: 10.1124/mol.109.062356
This article has not been copyedited and formatted. The final version may differ from this version.

FOOTNOTES

This work was supported by the National Institutes of Health Grants [NS58089, CA21765]; and the American Lebanese Syrian Associated Charities.

Portions of these data were previously presented in poster and talk formats at the CounterACT Network Research Symposium in Washington, DC in April 2009.

Reprint requests can be sent to:

Dr. Matthew R. Redinbo

Campus Box 3290

University of North Carolina at Chapel Hill

Chapel Hill, NC 27599-3290

redinbo@unc.edu

Molecular Pharmacology Fast Forward. Published on January 5, 2010 as DOI: 10.1124/mol.109.062356
This article has not been copyedited and formatted. The final version may differ from this version.

FIGURE LEGENDS

Figure 1. Organophosphate nerve agents and nerve agent analogs. Nerve agents contain a methyl, *O*-alkoxy, and good leaving group built on a central chiral phosphonate. The stereogenic OP nerve agent analogs contain a thiomethyl leaving group in place of the fluoride.

Figure 2. hCE1 Monomer. Each protein monomer has three domains; the α/β domain (blue) forms the trimer interface and caps the active site, the Regulatory region (orange) contains the secondary surface binding site (Z-site) and Glu354 of the catalytic triad, and the Catalytic domain (green) contains the central β-sheet conserved in serine hydrolases, as well as the two catalytic residues His468 and Ser221. There are two disulfide bonds (cyan), one in the α/β domain and the other in the catalytic domain, and one glycosylation site, at Asn79 (yellow).

Figure 3. hCE1-Cyclosarin Complex. A) Chemical scheme of hCE1 reacting with cyclosarin. **B**) Cut away view of the hCE1-cyclosarin active site. The catalytic triad and cyclosarin molecule are shown in purple, oxyanion hole in white, and the surrounding residues in green. Hydrogen bonds between the phosphoryl oxygen and the backbone nitrogen atoms in the oxyanion hole are shown in red.

Figure 4. hCE1-Cyclosarin Adduct Stereochemistry. Ser221 and His468 of the catalytic triad and the cyclosarin adduct are shown in purple. The oxyanion hole is colored white. **A**) Stereoview of a 3.1 Å resolution $F_o - F_c$ simulated annealing omit map (blue, contoured to 5 σ) calculated for the P_R-cyclosarin adduct. **B**) Stereoview of initial difference density maps for the incorrect P_S-cyclosarin adduct (green for positive, shown at 3 σ; red for negative, shown at -3 σ).

Figure 5. Bimolecular Rates of Inhibition (k_i) for hCE1 and Nerve Agent Analogs. Plotted as log k_i, hCE1 exhibits strong enantiomeric P_R preference for soman and cyclosarin analogs,

Molecular Pharmacology Fast Forward. Published on January 5, 2010 as DOI: 10.1124/mol.109.062356
This article has not been copyedited and formatted. The final version may differ from this version.

with only slight P_S sarin analog selectivity. Dissociation constants (K_d) are similar to authentic nerve agents, while phosphorylation rates (k_2) are 2-3 orders of magnitude slower. N=3, S.E.

Figure 6. hCE1 Reactivation after Inhibition by Racemic *bona fide* OP Nerve Agents or Stereospecific Nerve Agent Analogs. A) Spontaneous reactivation of racemic *bona fide* OP agents. Reactivation only occurs with sarin (■), with a half-time of reactivation of 45 hours (N=5, S.D.). Soman (●) and cyclosarin (◆) remained permanently inhibited. **B**) DAM-assisted reactivation with racemic *bona fide* nerve agents. Reactivation is only measured against sarin (■) with a half-time of reactivation of 41 minutes (N=3, S.E.). Soman (●) and cyclosarin (◆) did not reactivate. **C**) DAM-assisted reactivation of sarin analogs. The P_S isomer (■) reactivates with a half-time of 30 minutes (N=3, S.E.). P_R sarin (□) analog did not reactivate. **D**) DAM-assisted reactivation of soman analogs. Greatest reactivation was measured in the P_S (○) enantiomer, while the P_R (●) analog remained inhibited. **E**) DAM=assisted reactivation of cyclosarin analogs. Negligible reactivation was measured for either P_S (◇) or P_R (◆) cyclosarin analog. **F**) Determination of aging with P_S nerve agent analogs; no aging was measured for the P_S species.

Figure 7: hCE1-Sarin Model. A) P_R and P_S enantiomers of sarin modeled in the hCE1 active site. The *O*-isopropyl group on P_S sarin makes hydrophobic contacts with Phe101 and Leu97, while P_R does not have any additional interactions. **B**) Model of proposed mechanism of P_S sarin reactivation in hCE1. In AcChE, His468 has been observed to rotate away from Glu354 and interact with Glu221 after acylation. Modeling this shift in the hCE1 active site, there is an electronic network formed between Tyr152 (green) and His468 (yellow) that may either deprotonate Nε2 or allow Nδ1 of His468 to act as a general base for water activation. P_S sarin

Molecular Pharmacology Fast Forward. Published on January 5, 2010 as DOI: 10.1124/mol.109.062356
This article has not been copyedited and formatted. The final version may differ from this version.

(blue) was modeled into the hCE1-soman structure (RSCB PSB access code 2HRQ (Fleming et al., 2007)).

Molecular Pharmacology Fast Forward. Published on January 5, 2010 as DOI: 10.1124/mol.109.062356
This article has not been copyedited and formatted. The final version may differ from this version.

TABLE 1

Crystallographic data collection and refinement statistics

	Statistic
X-ray data collection	
Space group	$P2_12_12_1$
Cell dimensions	
a, b, c (Å)	55.6, 179.9, 200.6
α, β, γ (°)	90.0, 90.0, 90.0
Resolution (Å) (highest shell)	48-3.1 (3.3-3.1)[a]
R_{sym} (%)[b]	13.1 (48.1)
I/σ	13.6 (4.5)
Completeness (%)	97.5 (94.0)
Redundancy	7.0 (6.2)
Crystallographic refinement	
Resolution (Å)	48-3.1 (3.3-3.1)
Unique reflections	36,488
Mean thermal displacement parameter (Å^2)	
Protein	53.9
Water	49.2
RMSD	
Bond lengths (Å)	0.014
Bond angles (°)	1.70
R_{work}/R_{free} (%)[c,d]	26.6 (26.8)/29.9 (29.6)

Molecular Pharmacology Fast Forward. Published on January 5, 2010 as DOI: 10.1124/mol.109.062356
This article has not been copyedited and formatted. The final version may differ from this version.

[a]Number in parenthesis is for the highest shell.

[b] $R_{sym} = \Sigma|I - \langle I \rangle|\Sigma I$, where I is the observed intensity and $\langle I \rangle$ is the average intensity of multiple symmetry-related observations of that reflection.

[c] $R_{work} = \Sigma \, ||F_o| - |F_c|| \, / \, \Sigma|F_o|$, where F_o and F_c are the observed and calculated structure factors, respectively.

[d] $R_{free} = \Sigma \, ||F_o| - |F_c|| \, / \, \Sigma|F_o|$ for 7% of the data not used at any stage of structural refinement.

Figure 1.

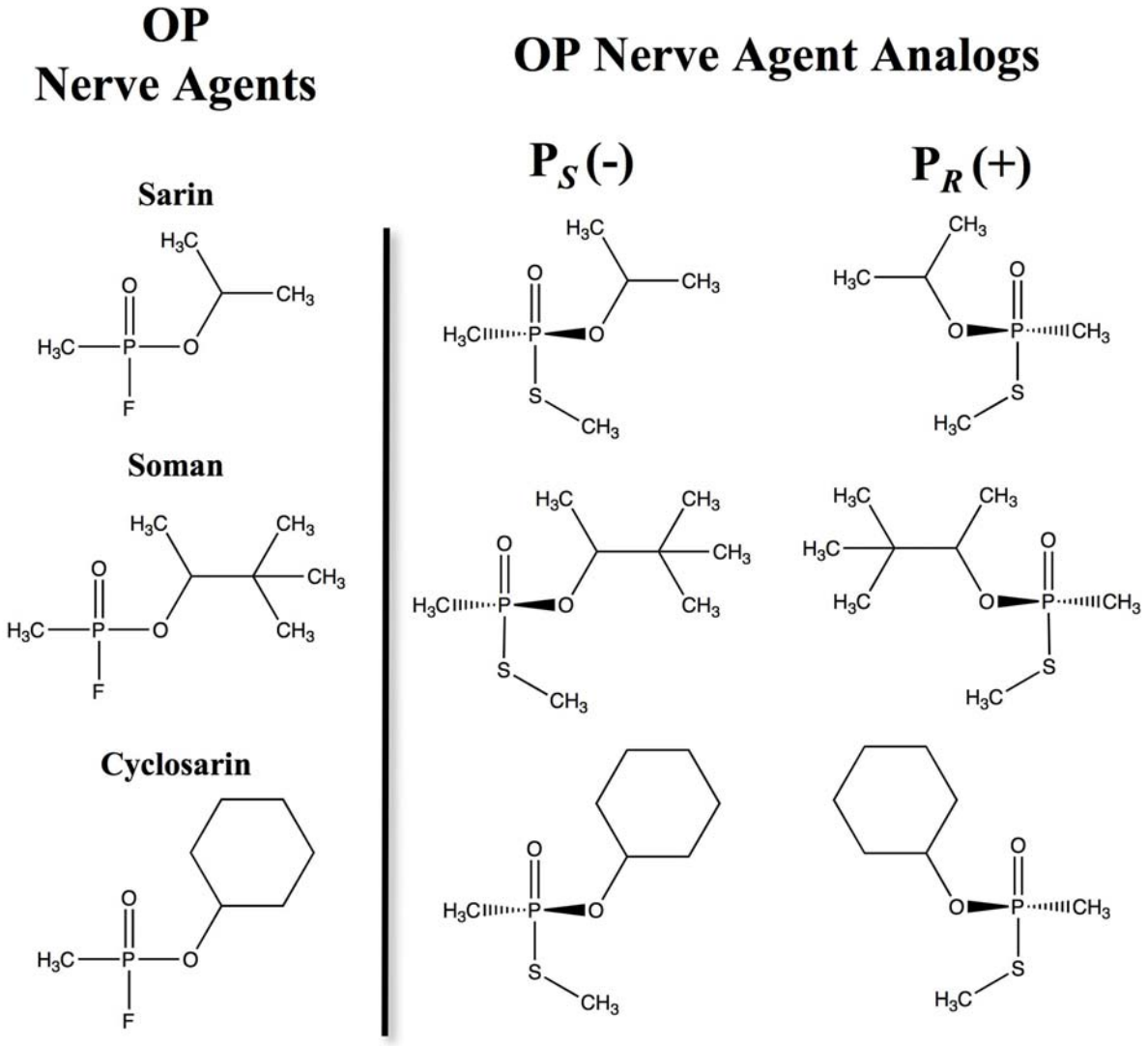

Figure 2.

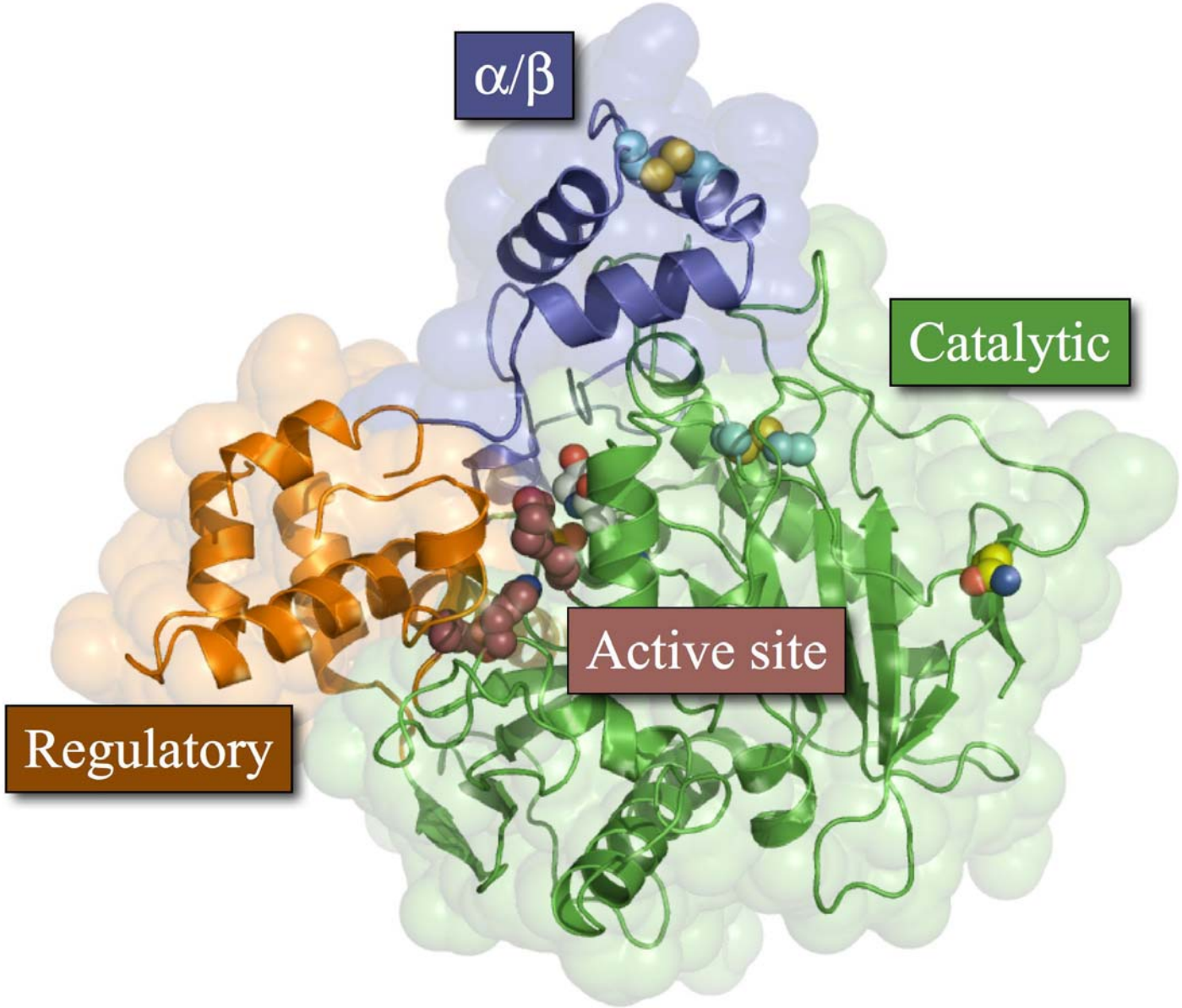

Figure 3.

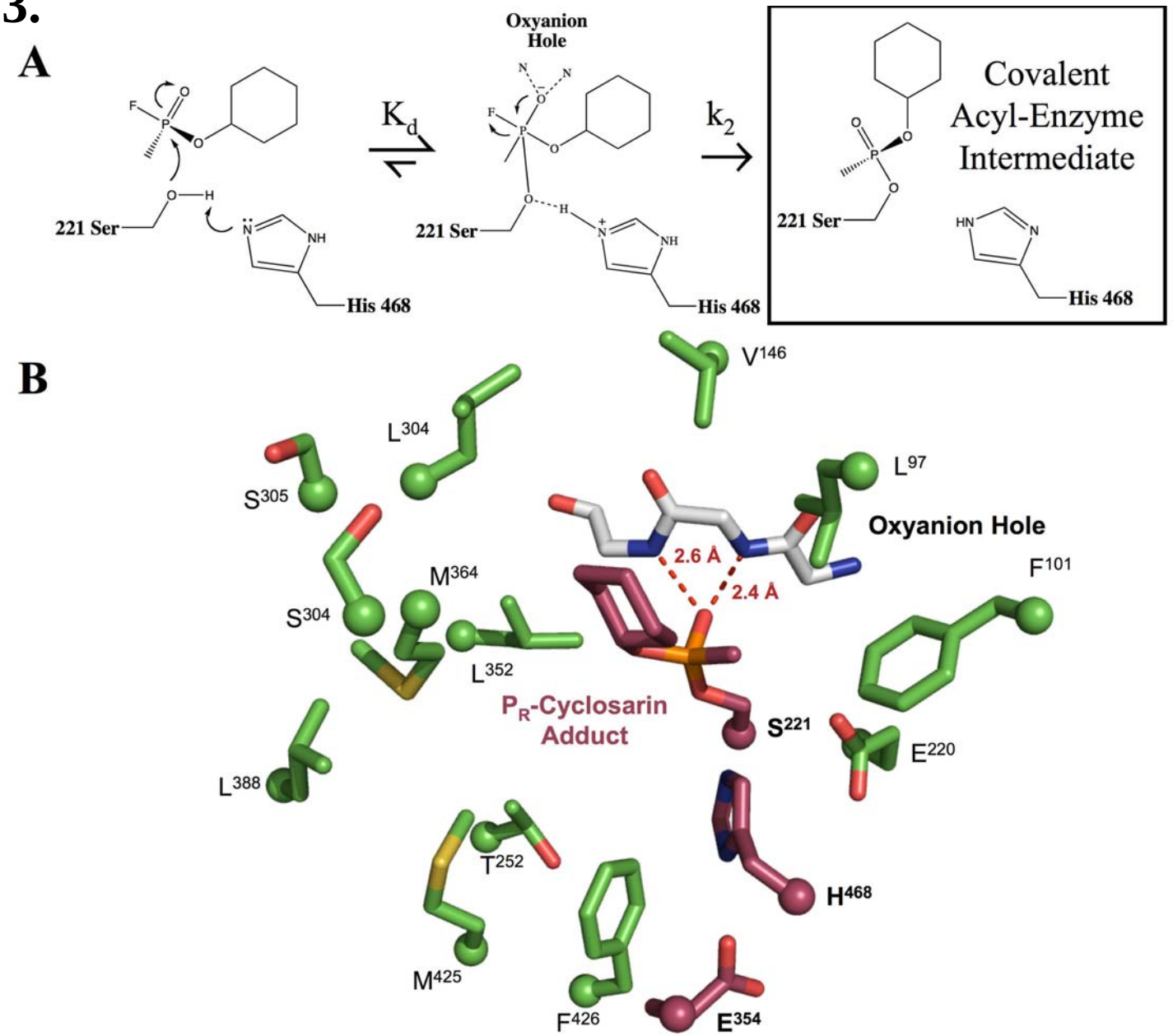

Figure 4.

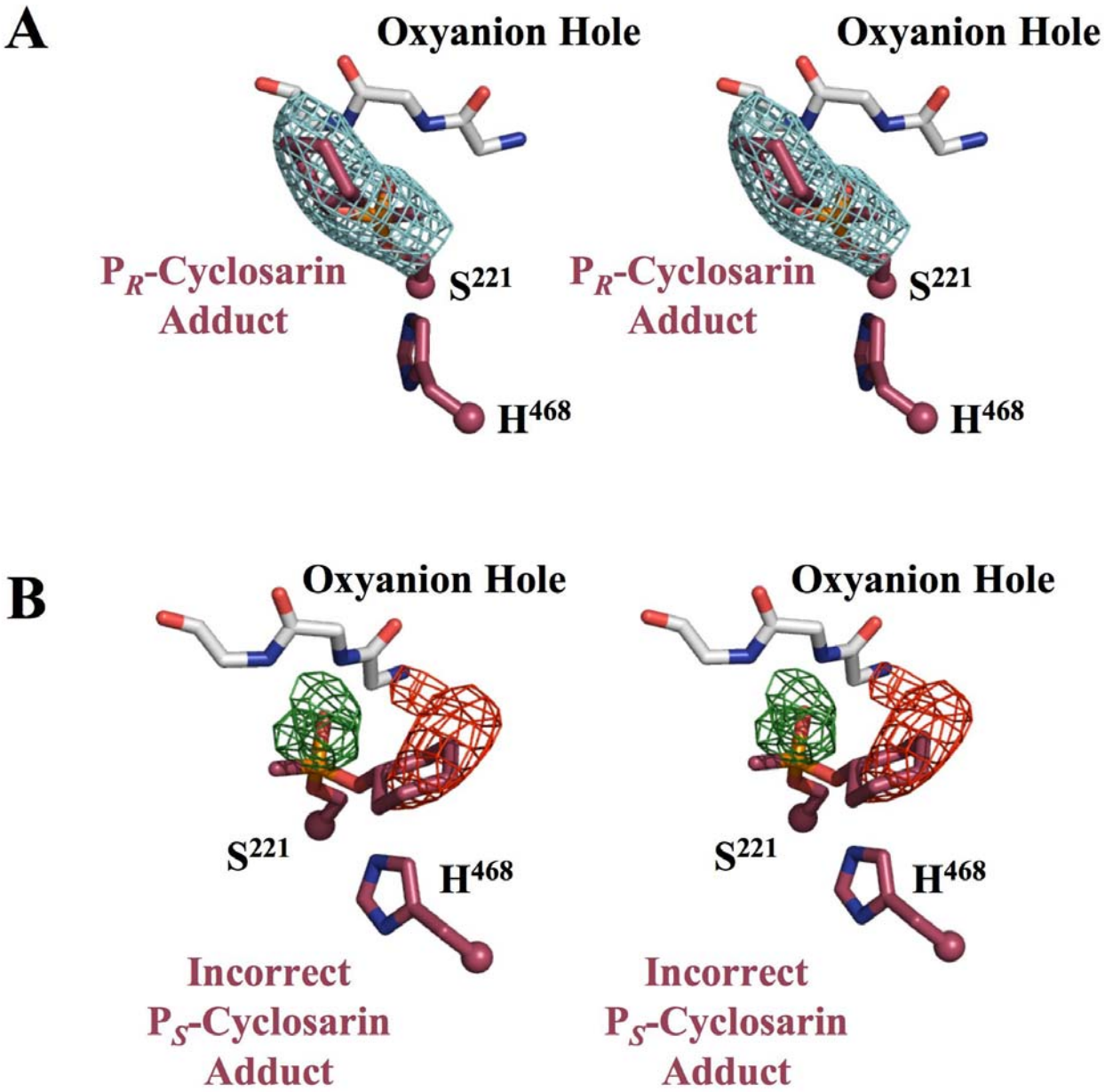

Figure 5.

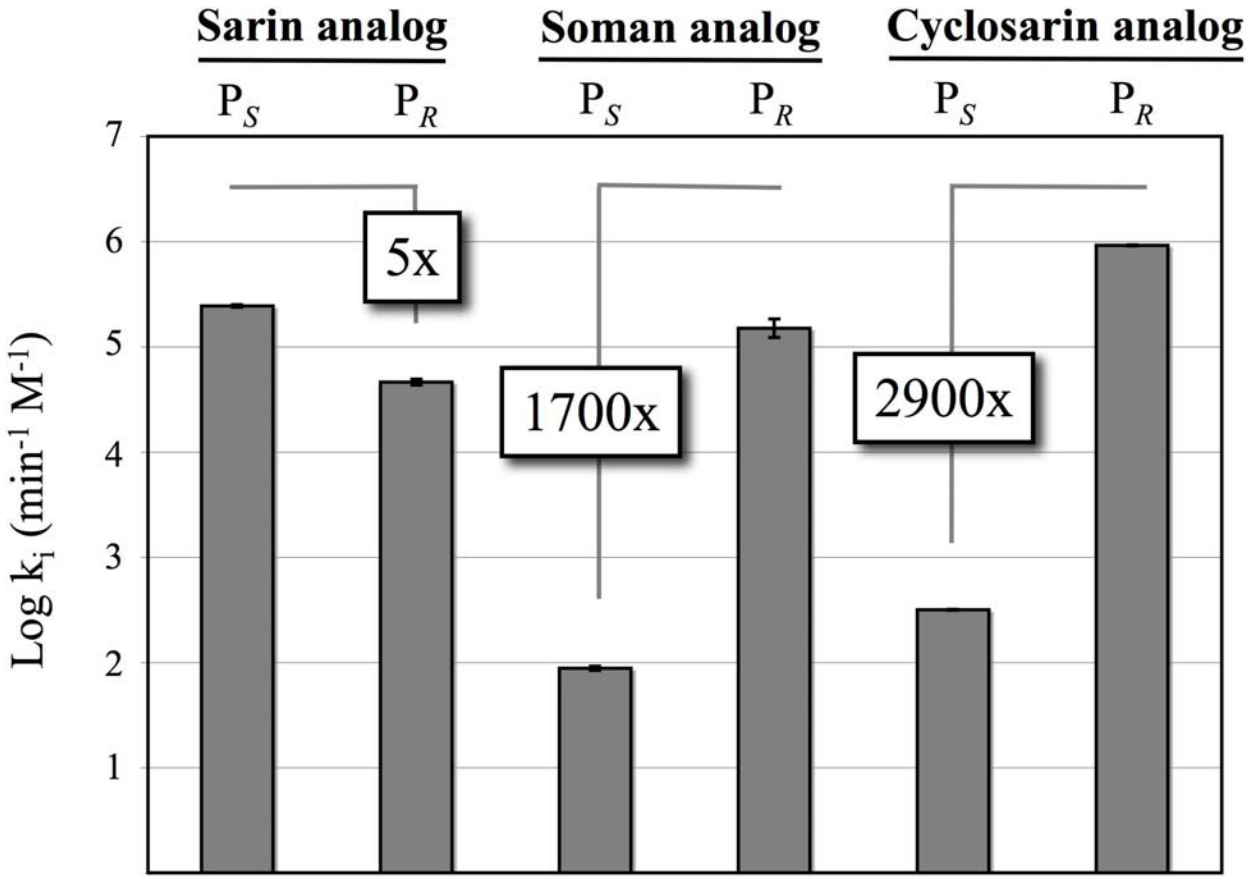

Analog Typ e		k_i (s^{-1} M^{-1})	K_d (M)	k_2 (s^{-1})	P_R/P_S
Sarin	P_S	$4.10 \pm 0.10 \times 10^{3}$	$3.70 \pm 0.20 \times 10^{-7}$	$1.53 \pm 0.02 \times 10^{-3}$	0.190
	P_R	$0.77 \pm 0.05 \times 10^{3}$	$1.40 \pm 0.20 \times 10^{-6}$	$1.12 \pm 0.01 \times 10^{-3}$	
Soman	P_S	1.46 ± 0.07	$8.00 \pm 2.00 \times 10^{-4}$	$1.20 \pm 0.01 \times 10^{-3}$	1705
	P_R	$2.50 \pm 0.50 \times 10^{3}$	$2.20 \pm 0.20 \times 10^{-7}$	$0.55 \pm 0.05 \times 10^{-3}$	
Cyclosarin	P_S	5.27 ± 0.07	$1.70 \pm 0.20 \times 10^{-3}$	$9.00 \pm 0.83 \times 10^{-3}$	2900
	P_R	$1.53 \pm 0.12 \times 10^{4}$	$3.20 \pm 0.10 \times 10^{-7}$	$5.30 \pm 0.50 \times 10^{-3}$	

Figure 6.

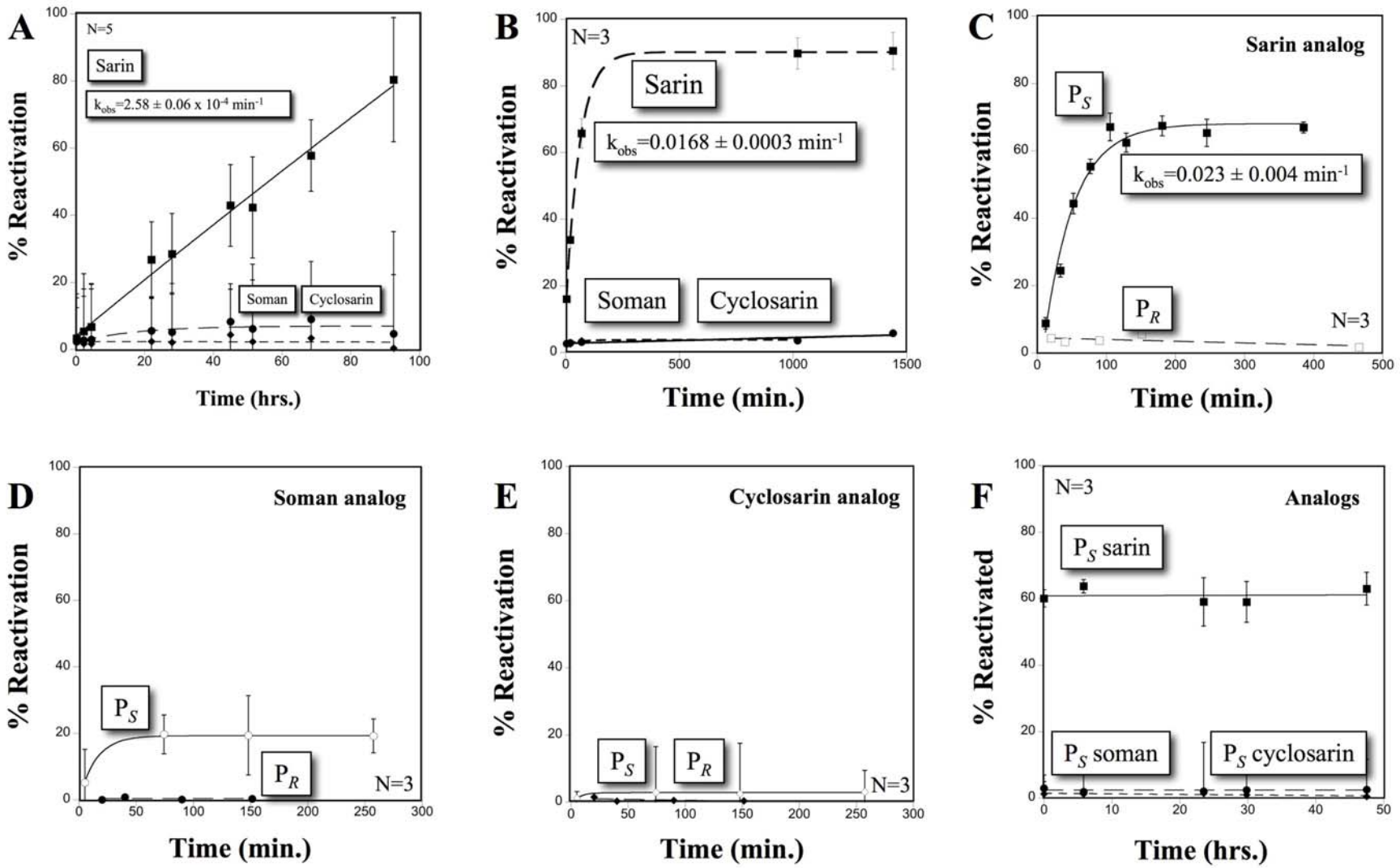

Figure 7.